RSC Advances

ROYAL SOCIETY OF CHEMISTRY

www.rsc.org/advances

RSC Advances

COMMUNICATION

Low-temperature catalytic decarboxylation of formic and acetic acid over Ru/TiO_2 catalyst: Prospects for continuous production of energy-rich gaseous mixtures

Received 00th January 20xx,
Accepted 00th January 20xx

DOI: 10.1039/x0xx00000x

www.rsc.org/

I. G. Osojnik Črnivec[a*], P. Djinović[a,b], B. Erjavec[a,b] and A. Pintar[a,b]

Catalytic decarboxylation is a novel and prospective pathway for continuous and efficient conversion of organic wastewaters. Stable conversion of acetic acid to CH_4 and CO_2 mixtures (T≥225 °C, S_p>80 %, 70 h TOS) was demonstrated. Approaches for overcoming catalyst deactivation during production of H_2-rich gas from formic acid are outlined.

In the last decades we are witnesses to continuously increasing energy consumption, accompanied by pertinent projections of fossil fuel reserves depletion. In the time period from 2000 to 2010, global energy use increased by 26 % and the reserves-to-production ratios for petroleum, gas and coal were recently estimated to be sufficient for the next 53, 55 and 112 years [1]. Industrial organic waste streams provide a possible alternative pathway for decreasing the dependence of fossil fuels by means of catalytic, thermochemical and biotechnological conversion processes. The ideal valorisation process will avoid the established total oxidation (such as biological oxidation based on activated sludge), and rather focus on procedures that enable energy extraction. For example, catalytic decarboxylation of carboxylic acids is a possible pathway for chemical and energetic valorisation of highly oxygenated organic contaminants, which is more beneficial than traditional purification technologies based on complete oxidation to CO_2 and H_2O.

Carboxylic acids are frequent constituents of various industrial wastewater streams, arising typically in textile, polymer, pulp and paper, tanning, food and beverage industries. Likewise, short-chain carboxylic acids, such as formic acid and acetic acid, are also common final products or intermediates of advanced oxidation processes [2,3]. High degree of oxygenation makes low carboxylic acids a very poor choice for liquid fuels due to their low energy content (5.4, 13.5 and 44 MJ/kg LHV for formic, acetic acid and gasoline, respectively). Therefore, it is highly advantageous to catalytically convert them under mild conditions into chemical intermediates (such as H_2, CO, CO_2 and CH_4), which allow for further chemical transformation into useful products using well established routes [4]. Decarboxylation of formic acid (reaction 1; $\Delta H°_{298\ K}$ = -29.3 kJ/mol) produces H_2 and CO_2, whereas decarboxylation of acetic acid (reaction 2; $\Delta H°_{298\ K}$ = -8.6 kJ/mol) produces CH_4 and CO_2.

$$HCOOH_{(l)} \rightarrow CO_{2(g)} + H_{2(g)} \quad (1)$$

$$CH_3COOH_{(l)} \rightarrow CH_{4(g)} + CO_{2(g)} \quad (2)$$

Studies of catalytic short-chain carboxylic acid valorisation focus mostly on high-temperature (T_r>600 °C) steam reforming process. This reaction is, despite the large water surplus in the feed (water/acid=10/1), plagued by severe carbon deposition and fast catalyst deactivation [5,6]. On the other hand, reports on catalytic decarboxylation process, which is operated at mild conditions in the continuous-flow mode, are very scarce and either based on mechanistic aspects [7] or operation in batch mode [8]. Previously, Pintar et al. [9] performed a study on catalytic wet-air oxidation of various organic pollutants (phenol, formic and acetic acid) in a trickle-bed reactor between 55–250 °C, where complete oxidation of formic acid, complete removal of phenol and partial oxidation of acetic acid were observed. However, they also observed that in inert He atmosphere either total or partial conversion of formic and acetic acid occurred over Ru/TiO_2 catalyst, and the amount of gaseous decomposition products could not be quantified due to low reactant concentration (2 g/L). This sparked research activities that are reported in this study; namely, we demonstrate the possibility of continuous low-temperature decarboxylation of aqueous solutions containing acetic (AA) and formic acid (FA) in a three-phase trickle-bed reactor with the aim to produce CH_4, H_2 and CO_2. Also, the window of relevant operating conditions was established and the network of competing side reactions is analysed and discussed. Experimental details are given in the supplement.

Tests confirmed negligible contribution of TiO_2 support to the studied reactions (at the studied reaction conditions X_{feed/TiO_2}<1 %). For reactions (1) and (2), calculated equilibrium carboxylic acid conversions were above 99.9 % (using Gaseq 0.79 software) in the 50–300 °C and 1–50 bar range, meaning they are not equilibrium limited. Theoretically achievable gas-phase concentrations of H_2 and CH_4 at 100 % decarboxylation selectivity as a function of acid concentration and its conversion are provided in Fig. S1.

[a] Laboratory for Environmental Sciences and Engineering
National Institute of Chemistry
Hajdrihova 19, SI-1001 Ljubljana, Slovenia
[b] Centre of Excellence for Low Carbon Technologies
Hajdrihova 19, SI-1001 Ljubljana, Slovenia
* v corresponding author (e-mail: gasan.osojnik@ki.si)
Electronic Supplementary Information (ESI) available.
See DOI: 10.1039/x0xx00000x

Initial tests were performed with a low concentration of carboxylic acid feed (c=2 g/L) to define the corresponding windows of operation. Catalytic decarboxylation of FA was observed already at 70 °C (10 % conversion), reaching full conversion at temperatures of 180 °C (Fig. 1a). TOC analysis showed no organic residue remaining in the aqueous phase at full FA conversion.

During FA conversion at T<165 °C, H_2 and CO_2 were identified as reaction products, confirming decarboxylation as the only occurring reaction. At T>165 °C, CO was also detected as the reaction product, indicating participation of H_2 and CO_2 (FA decarboxylation products) in the simultaneous reverse water gas shift (RWGS) side reaction (reaction 3; $\Delta H°_{298\,K}$ = 41.0 kJ/mol).

Upon increasing FA concentration in the feed (c=10 g/L), its full conversion were reached at slightly higher temperature (195 °C and above, test FT10, Fig. S2a) due to the kinetic effect. At these temperatures, CO_2 and traces of CO (195–210 °C) and CH_4 (195–240 °C) were identified in the gas phase. H_2 could not be confirmed due to being consumed in the RWGS reaction (to generate CO), as well as CO and CO_2 hydrogenation reactions which represent the origin for methane (reactions 4 and 5; $\Delta H°_{298\,K}$ = -206.2 and -164.9 kJ/mol, respectively).

$$H_2 + CO_2 \leftrightarrow CO + H_2O \quad (3)$$

$$CO_{2(g)} + 3H_{2(g)} \leftrightarrow CH_{4(g)} + H_2O_{(l)} \quad (4)$$

$$CO_{2(g)} + 4H_{2(g)} \leftrightarrow CH_{4(g)} + 2H_2O_{(l)} \quad (5)$$

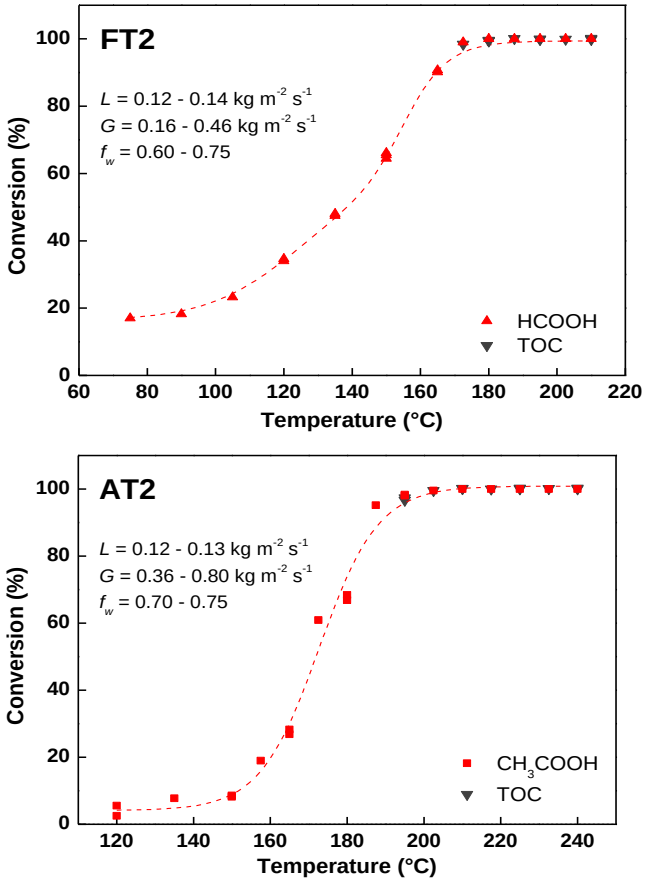

Figure 1. Conversion of (FT2) formic acid and (AT2) acetic acid at feed concentration of 2 g/L as a function of temperature over 3 wt. % Ru/TiO_2 catalyst. The TOC conversion and the range of hydrodynamic parameters (f_w – wetted fraction or wetting efficiency, G – gas mass velocity, L – liquid mass velocity) are presented as well.

Due to partial wetting of the catalyst (60–75 %) in the trickle-bed at the employed reaction conditions (hydrodynamic parameters are denoted in Fig. 1 and presented in detail in Fig. S3), the products of FA decarboxylation reaction (H_2 and CO_2) were exposed to the Ru/TiO_2 surface, enabling the occurrence of subsequent gas-phase transformations, such as RWGS, CO and CO_2 methanation reactions, especially Ru/TiO_2 and Ru/CeO_2 have been previously identified to initiate CO methanation reaction at temperatures as low as 150 °C, with CO_2 starting to contribute at about 190 °C [10]. Up to our knowledge, this is the first time that CO and CO_2 methanation reactions were observed to take place in a three-phase trickle-bed reactor.

During the 50 h long-term FA decarboxylation test at 180 °C (c = 10 g/L, test FS10, Fig. S2b), a continuous catalyst deactivation was observed (FA conversion decreased from 100 to 75 %, accompanied with a continuous drop of CO_2 concentration from 2 to 0.5 %). The deactivation can be attributed to the accumulation of carbonaceous deposits on the catalyst surface and blocking of active sites, as will be discussed later on. When catalyst stability was investigated using a FA concentration of 20 g/L (T_r=225 °C), a continuous deactivation was noticed with a simultaneous decrease of CO_2, CO and CH_4 concentrations (Fig. S4). At the beginning of the test, 5.9 % CO_2 was produced, decreasing to 4.9 % after 4 hours of operation (SCO2-225 °C=58 %). By taking into account all the recorded mass fluxes, over 90 % carbon mass balance was achieved, confirming good experimental determination of the studied system (e.g. for AT10 test, 92 wt. % of C mass balance was accounted for by the following weight fractions: C_{feed}=1, $C_{effluent}$=0.26, C_{gas} =0.62, $C_{deposits}$=0.04).

With AA feed of 2g/L, decarboxylation did not occur until 120 °C. Its complete conversion and total removal of organic carbon from the liquid phase were achieved at temperatures above 210 °C (Fig. 1b). Importantly, methane and CO_2 were observed as the only reaction products in the whole investigated temperature range. Besides unconverted AA, no other organic compounds could be identified in the liquid phase. Upon increasing the AA concentration to 10 g/L, high conversion (95 %) was achieved at 225 °C, yielding a roughly equimolar mixture of CH_4 and CO_2 ($n(CH_4)/n(CO_2)$=1.13/1), while no other gaseous products were detected (Fig. 2a). Higher solubility of CO_2 in the aqueous phase most likely contributes to an apparent methane surplus in the gas phase. Similarly to the experiment with FA, higher temperatures were required also for achieving full AA conversion due to its higher concentration in the feed (test AT10, Fig. 2a). It is encouraging to note that no catalyst deactivation was observed during long-term (70 h TOS) decarboxylation of 10 g/L AA at 225 °C (test AS10, Fig. 2b). By increasing the AA feed concentration to 20 g/L at 225 °C, stable decarboxylation of AA (complete conversion and $S_{CH_4\text{-}225\ °C}$=80 %) was maintained for the whole duration of the experiment (4 h), yielding 5.1 vol. % of CH_4 and 5.4 vol. % of CO_2 (as depicted in Fig. S4). No side reactions were observed during AA decarboxylation as the reaction temperature is too low for CH_4 activation over the catalyst used.

Morphological properties of TiO_2 support (Table 1) were not altered after Ru impregnation, drying and catalyst stabilization. The adsorption-desorption analysis of the prepared materials reveal: (i) characteristic type III (IUPAC) isotherms, indicating the presence of a mesoporous structure and (ii) an extended pore size distribution range (5–100 nm), suggesting the well-developed pore structure o

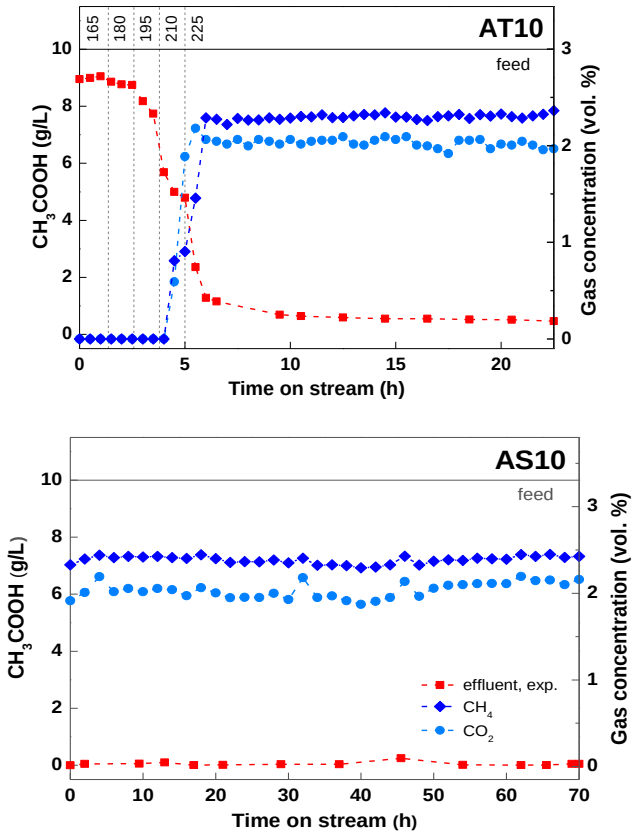

Figure 2. Conversion of acetic acid at feed concentration of 10 g/L at (AT10) T_r=165–225 °C and (AS10) T_r=225 °C. Outlet gas phase composition is also shown.

the catalyst does not constrain the occurrence of the studied reaction (e.g. AA molecule size is 0.4 nm). Furthermore, catalyst exposure to hydrothermal reaction conditions during decarboxylation experiments FT10 and AS10 did not alter their morphology beyond the measurement uncertainty value, which is about 5 %.

In the case of test runs, FS10 and AT10, the observed decrease of BET surface area could be attributed to carbon accumulation, as the highest amounts of deposits were accumulated on the surface of these two materials.

All diffraction peaks (XRD patterns shown in Fig. S5) in the analysed samples could be attributed to the crystalline structure of anatase (PDF 00-021-1272) and rutile (PDF 01-089-0552). Exposing the catalysts to hydrothermal conditions and temperatures above 180 °C (runs FT10, AT10, and AS10) initiated a partial phase transition of anatase into thermodynamically more stable rutile. The most apparent rutile enrichment (from 30 to 39 %) was evident after the longest test run (70 h at 225 °C), also reflecting in the change of average domain size of rutile and a slight decline in BET surface area of the catalyst, while simultaneously preserving the apparent catalyst surface morphology (Fig. S6). During tests FS10 and AT10, accumulation of carbon-rich deposits (0.3–6.1 wt. %) was detected over the catalyst. As can be seen in Fig. S2b and Table 1, a high degree of catalyst deactivation during test FS10 coincides with the highest amount of carbon deposits. To gain further insight into the nature of the carbonaceous deposits, DRIFTS and TPO (temperature programmed oxidation) analyses were performed.

DRIFTS spectra of all analysed samples (Fig. 3) are dominated by a broad band centered at 940 cm^{-1}, which originates from stretching and bending vibrations of Ti–O–Ti bonds [13]. Samples analysed prior to thermal treatment (fresh TiO_2 and impregnated and dried Ru/TiO_2) also produce a very broad feature between 3600 and 2600 cm^{-1}, which is associated with the stretching vibrations of hydrogen-bonded surface water molecules and various hydroxyl groups [14,17].

Weak bands at 3694 and 3617 cm^{-1} can be assigned to stretching modes of non-hydrogen-bonded -OH groups [16]. In addition, a peak of varying intensity can be observed at 1630 cm^{-1}, which is assigned to the bending mode of water. These bands together indicate significant hydration of the TiO_2 catalyst surface.

Carbonate (C–O) stretching bands at 1540 and 1464 cm^{-1} were also observed in TiO_2 and Ru/TiO_2 samples before the reaction. Bending C–O vibrations of these species which, expected between 1100 and 1000 cm^{-1} and about 850 cm^{-1} [17], could not be identified as they are overwhelmed by the dominant Ti–O–Ti bond vibrations. Carbonate species are formed due to the interaction of lattice oxygen/hydroxyl species with atmospheric CO_2 when exposed to air. On Ru/TiO_2 catalysts analysed after the temperature programmed FA (FT10) and isothermal AA (AS10) decomposition experiments, no additional bands compared to fresh samples could be seen, showing no accumulation of carbon species on the catalyst. This is in line with the C elemental analysis of spent samples (these show up to 0.4 wt. % C) and also previous results reporting that carbonaceous deposits originating from AA decomposition can be removed from the catalyst surface at temperatures above 230 °C [9].

Similar effect was observed for FA, as operation at 240 °C in the last step of the FT10 test run resulted in no accumulation of carbonaceous deposits. On the other hand, additional peaks at 2980, 2940, 2880, 1686, 1473 and 1464 cm^{-1} can be observed after the FS10 and AT10 tests. These can be assigned to symmetric and asymmetric stretching modes of $-CH_2-$, $-CH_3$ and C=O bonds, and reveals the structure of carbonaceous deposits is paraffinic and oxygenated (such as acids, aldehyde and esters).

The deposits originate from AA and FA and reactions between such adjacent surface species (dehydration, polymerization, etc.). Decomposition products of AA (CH_4, CO_2) are probably not active precursors for the formation of hydrocarbons that remain adsorbed

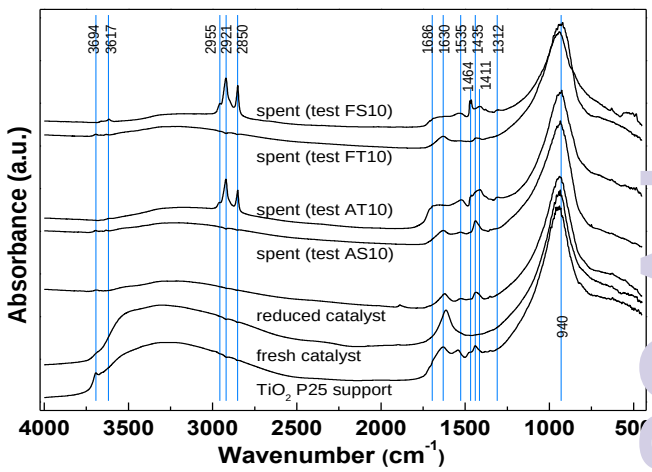

Figure 3. DRIFTS spectra of TiO_2 support and Ru/TiO_2 catalysts before and after FA and AA decarboxylation reactions.

Table 1. Morphological properties of bare TiO_2 P25 support and 3 wt. % Ru/TiO_2 catalysts: BET surface area (S_{BET}), total pore volume and pore diameter (V_{PT} and d_{PT}), average domain size of TiO_2 polymorphs (anatase - d_{101}, rutile - d_{110}), weight fraction of anatase in TiO_2 ($w_{anatase}$) and amount of accumulated carbon (w_C).

Sample	S_{BET} (m^2/g)	V_{PT} (cm^3/g)	d_{PT} (nm)	d_{101} (nm)	d_{110} (nm)	$w_{anatase}$ (wt. %)	w_C (wt. %)
Bare TiO_2 P25	47.3	0.32	27.0	26.5	46.6	72	0.3
Fresh catalyst	47.2	0.30	25.4	27.1	48.3	70	0.1
Reduced catalyst	48.3	0.31	25.5	27.4	45.3	70	0.1
Spent catalyst (test FT10)	45.5	0.30	26.2	32.0	54.4	66	0.3
Spent catalyst (test FS10)	26.4	0.23	34.1	30.4	49.8	71	6.1
Spent catalyst (test AT10)	32.4	0.27	33.0	31.5	50.7	67	2.9
Spent catalyst (test AS10)	42.7	0.29	27.4	33.8	55.7	61	0.4

on the catalyst despite the fact that Ru/TiO_2 is active for hydrogenation and carbon chain growth through Fischer-Tropsch chemistry, when using syngas to produce larger hydrocarbons [18]. The reason is twofold: (i) reaction temperature is too low for catalytic C-H bond cleavage in methane, which would enable CO_2 hydrogenation in case of AA decarboxylation (where CO_2 and CH_4 are exclusive products); (ii) if Fischer-Tropsch chemistry was occurring, this would be observed during continuous GC and HPLC analyses.

A combination of C elemental analysis and TPO results revealed 63 wt. % carbon content (the rest is O and H) in accumulated deposits after AT10 test (Δm_{TPO}=4.6 wt. % vs. 2.9 wt. % C) indicating their highly oxygenated structure, likely originating from strong adsorption of reactants and intermediates, possibly undergoing polymerization during operation at temperatures below 225 °C. When long-term isothermal test at 225 °C was performed (test AS10), no accumulation of carbonaceous species was noticed, as the reaction temperature was high enough to facilitate their desorption from the catalyst surface (notice the overlap of both decarboxylation reaction and desorption temperature windows, Fig. S7). On the contrary, carbon deposits containing 91 wt. % C were found on the spent catalyst after FA decarboxylation (test FS10, Δm_{TPO}=6.7 wt. % vs. 6.1 wt. % C) indicating their much less oxygenated composition compared to AT10 experiment with AA. This is in line with less intense IR absorption band at 1686 cm^{-1} (C=O bond) in sample FS10 compared to AT10 (Fig. 3). Higher temperature, required for removal of carbon deposits (247 and 285 °C for AT10 and FS10, respectively, Fig. S7), resulted in their accumulation during catalytic decarboxylation of FA at 225 °C. In both cases, only endothermic peaks were identified during TPO-DSC analysis of spent catalyst samples (Fig. S7), which implies that accumulated carbonaceous deposits were essentially removed by desorption instead of combustion.

To conclude, low-temperature catalytic decarboxylation of AA in a trickle-bed reactor over 3 wt. % Ru/TiO_2 was demonstrated (X_{AA}<98 %, S_{CH_4}>80 %). At reaction temperatures below 225 °C where incomplete AA conversion is achieved, accumulation of highly oxygenated carbonaceous deposits is observed over the catalyst, leading to a continuous deactivation. At 225 °C and AA concentrations up to 20 g/L, complete conversion was achieved and no carbonaceous residues accumulated over the catalyst, resulting in stable catalyst operation and roughly equimolar CH_4 and CO_2 product stream obtained during 70 h TOS. In case of FA decarboxylation, lower selectivities (X_{FA}<100 %, S_{CO_2}<60 %) compared to AA were achieved. Continuous deactivation of the catalyst was observed at FA concentration of 10 g/L and 180 °C due to accumulation of thermally stable carbonaceous residue which blocks the catalytically active sites. These deposits were removed by temperature programmed desorption at 285 °C. Besides decarboxylation reaction, simultaneous occurrence of RWGS and CO/CO_2 methanation reactions was observed, which shifted the product spectrum from H_2 and CO_2 to CH_4, CO and CO_2.

The presented work demonstrates an efficient pathway for stable and continuous low-temperature AA conversion into CH_4 and CO_2. Efficient decarboxylation of FA into H_2 and CO_2, however, still requires a catalyst with suppressed activity for the identified side reactions at sufficiently high reaction temperatures, which are needed for continuous desorption of carbonaceous deposits that would in turn enable stable catalytic activity.

Acknowledgements

Authors gratefully acknowledge financial support of the Ministry of Education, Science and Sport of the Republic of Slovenia (Research program P2-0150) and the European Social Fund (Operational Programme for Human Resources Development 2007–2013).

Notes and references

1 BP Statistical Review of World Energy June 2014, BP p.l.c., London, 2013 <bp.com/statisticalreview> 4. March 2015.
2 F. Arena, C. Italiano, A. Raneri, C. Saja, *Appl.Catal. B,* 2010, **99**, 321.
3 B. Erjavec, R. Kaplan, P. Djinović, A. Pintar, *Appl.Catal. B*, 2013, **132-133**, 342.
4 P. Djinović, I.G. Osojnik Črnivec, B. Erjavec, A. Pintar, *ChemCatChem*, 2014, **6**, 1652.
5 A.C. Basagiannis, X.E. Verykios, *Appl.Catal. A*, 2006, **308**, 182.
6 P. Mohanty, M. Patel, K.K. Pant, *Bioresour.Technol.*, 2012, **123**, 558.
7 C. Hu, S.W. Ting, J. Tsui, K.Y. Chan, *Int.J.Hydrogen Energ.*, 2012, **37**, 6372.
8 T. Nozawa, Y. Mizukoshi, A. Yoshida, S. Naito, *Appl.Catal. B* 2014, **146**, 221.
9 A. Pintar, J. Batista, T. Tišler, *Appl. Catal. B*, 2008, **84**, 30.
10 P. Djinović, C. Galletti, S. Specchia, V Specchia, *Catal.Today*, 2011, **164**, 282.
11 P. Djinović, I.G. Osojnik Črnivec, J. Batista, J. Levec, A. Pintar, *Chem. Eng. Process.*, 2011, **50**, 1054.
12 P. Panagiotopoulou, D.I. Kondarides, X.E. Verykios, *Catal.Today*, 2012, **181**, 138.
13 V. Štengl, S. Bakardjieva, J. Šubrt, E. Večerníková, L. Szatmary, M. Klementová, V. Balek, *Appl.Catal. B*, 2006, **63**, 20.
14 M. Burgos, M. Langlet, *Thin Solid Films*, 1999, **349**, 19.
15 S. Kataoka, M.I. Tejedor-Tejedor, J.M. Coronado, M.A. Anderson, *J. Photochem. Photobiol. A*, 2004, **163**, 323.
16 M. Primet , P. Pichat , M.V. Mathieu, *J.Phys.Chem.*, 1971, **75**, 1216.
17 S. Agarwal, X. Zhu, E.J.M. Hensen, L. Lefferts, B.L. Mojet, *J.Phys.Chem. C*, 2014, **118**, 4131.
18 T. Komaya, A.T. Bell, *J.Catal.*, 1994, **146**, 237.

